

Vehicle Following On A Ring Road Under Safety Constraints: Role of Connectivity and Coordination

Milad Pooladsanj, Ketan Savla, and Petros A. Ioannou

Abstract

A fundamental problem in traffic networks is driving under safety and limited physical space constraints. In this paper, we design longitudinal vehicle controllers and study the dynamics of a system of homogeneous vehicles on a single-lane ring road in order to understand the interplay of limited space, speed, and safety. Each vehicle in the system either operates in the cruise control mode or follows a vehicle ahead by keeping a safe time headway. We show that if the number of vehicles is less than a certain critical threshold, vehicles can occupy the limited space in many different configurations, i.e., different platoons of different sizes, and they converge to a uniform maximum speed while attenuating errors in the relative spacing upstream a platoon. If the number of vehicles exceeds the threshold, vehicles converge to a unique symmetric configuration and the equilibrium speed decreases as the number of vehicles increases. Next, we consider vehicle-to-vehicle (V2V) communication and show that it increases the critical number of vehicles that can travel with the maximum speed. Finally, we consider central coordination and show that the proposed controllers can force vehicles to converge to a desired configuration specified by the coordinator while maintaining safety and comfort. We demonstrate the performance of the proposed controllers via simulation.

I. INTRODUCTION

Traffic congestion has costed billions of dollars, hours, and gallons of fuel in the past years [1]. While this congestion is a direct consequence of high travel demand competing to utilize the limited supply of road networks in a safe manner [2], [3], it is magnified by poor human drivers' response to various disturbance [4]. It has been reported that Connected and Autonomous Vehicles (CAVs) have the potential to compensate for human errors and corresponding delays to effectively improve the throughput and capacity of highways [4]. However, the analysis of the limited capacity of road networks, which we shall refer to as *bounded space*, in conjunction with safety constraints has received little attention in microscopic traffic studies of CAVs.

The impact of CAVs on traffic flow in the longitudinal direction is often evaluated by considering autonomous vehicles on an unbounded single lane road with no passing. The majority of research in this direction consider a platoon of vehicles and assume that the leader of the platoon follows a desired speed trajectory. The objective is then to design state-feedback throttle/brake controllers for the following vehicles such that they can adjust their speed to the speed of the leader while keeping a safe distance from the next vehicle [5], [6]. The dynamical analysis of the following vehicles provide results on collision avoidance, attenuation of errors upstream the platoon, the effect of delay in the system performance, ride comfort, and the impacts of integration of communication channels [5]–[15]. The aforementioned research efforts aim their attention at evaluating the performance of CAVs when they are already in the vehicle following mode. In practice, the performance of CAVs in handling different situations such as switching between different modes of operation must be also taken into account. In [16], a supervisory controller was designed and analyzed which was responsible for interacting with the throttle/brake controller, choosing the proper mode of operation, e.g., cruise control or vehicle following, and the transition between these modes, and detecting any irregular behavior such as an emergency stopping situation. In all of these studies, however, increasing the number of vehicles does not affect the speed or density since an infinite space is assumed. In other words, the aforementioned analyses describe, at best, the behavior of CAVs under the safety constraint but not the space constraint.

The analytical understanding of the interplay between the safety constraint, speed limit, and space limitation by using a simple road geometry will help analyze these effects for more complicated road geometries and networks where space is limited. A simple, but practical, such setup is a ring road. In the experiment described in [17], a single lane ring road was used to show the formation of stop-and-go waves when all vehicles are human-driven and there is no bottleneck. Inspired in part by [17], there has recently been dynamical analysis on this setup for mixed-autonomy settings [18]–[20]. The foci of the analytical aspects of these works, however, is on the formation and dissipation of traffic jams using autonomous vehicles for a high density scenario, without explicit consideration of safety. Earlier work from the authors [21] explicitly included the safety constraint for a simple vehicle model. However, the impact of V2V communication and central coordination of vehicles on the bounded space was not addressed. Practical bounds on the acceleration of vehicles was not considered either.

M. Pooladsanj and P. A. Ioannou are with the Department of Electrical Engineering, University of Southern California, Los Angeles, CA 90007 USA (e-mail: (pooladsa@usc.edu; ioannou@usc.edu).

K. Savla is with the Sonny Astani Department of Civil and Environmental Engineering, University of Southern California, Los Angeles CA 90089 USA (e-mail: ksavla@usc.edu). K. Savla has financial interest in Xtelligent, Inc.

This work was supported in part by NSF CMMI 1636377 and METRANS 19-17.

In this paper, we consider homogeneous automated vehicles on a closed single lane ring road. We adopt a nonlinear vehicle model with first-order engine dynamics from [22] derived from Newton's second law of motion. We design state-feedback control laws based on feedback linearization to control the throttle and brake commands. Three different scenarios are considered. In the first scenario, we assume that vehicles do not communicate and there is no coordination. Each vehicle either follows a constant speed trajectory, i.e., is in the cruise control mode, or safely follows the vehicle ahead, i.e., the vehicle following mode, by keeping a safe headway. Transitioning between modes of operation is determined by a combination of relative spacing and speed signals and is handled by the vehicle's supervisory controller as discussed in [16]. It is analytically shown that the equilibrium of this dynamical system leads to the well-known triangular fundamental diagram. In other words, the interplay of bounded space, speed limit, and safety can be quantified in a straightforward manner with this problem formulation. We explicitly characterize the critical density ρ_c of the fundamental diagram, at which the flow is maximized, in terms of system parameters (time headway constant, free flow speed, minimum standstill safety distance, and length of each vehicle). In the second scenario, we assume that vehicles are also able to communicate their braking capabilities and their instantaneous acceleration with their immediate predecessor. We show that V2V communication increases ρ_c and the capacity of the road compared to the first scenario, thus it enhances the free flow region of the fundamental diagram. In the final scenario, we assume that a central coordinator communicates the desired platoon formations and inter-platoon spacings to certain vehicles. We prove that the designed controllers guarantee robust speed tracking and/or vehicle following, and attenuation of errors in the desired relative spacing, speed, and acceleration upstream a platoon while satisfying desired acceleration bounds for all three scenarios. We demonstrate the performance of the controllers by simulating different scenarios.

The contributions of this paper can be summarized as follows:

- 1) We illustrate the utility of a ring road setup to analyze the impact of space limitation, speed limit, safety constraint, and V2V communication on flow and density in a straightforward manner;
- 2) We show that when every vehicle seeks to attain the maximum possible speed while respecting speed limit and safe distance to the vehicle in front, then the emergent configuration of inter-vehicle spacing is unique at high density but not at low density;
- 3) We describe a protocol by which a central coordinator can safely achieve a desired configuration at low density.

The rest of the paper is outlined as follows. In section II, we state the problem formulation and control objectives. In Section III, we first consider the case where vehicles do not communicate and there is no coordination on the ring road. We next extend the analysis for the case where V2V communication is possible. In Section IV, the role of central coordination on the ring road is evaluated and suitable transition logic are proposed. Section V provides simulation results for these scenarios. We conclude the paper and discuss future directions in section VI.

II. PROBLEM FORMULATION

A. Basic Notations

Consider n homogeneous vehicles of length L , on a closed ring road. Without loss of generality, assume that the perimeter of the ring road is P for some $P > nL$. We assign coordinates over the distance interval $[0, P]$ to the ring road in the clock-wise direction. Let $\mathcal{N} = \{1, 2, \dots, n\}$ be the set of vehicles' indices, where vehicle i is the i^{th} -closest vehicle to point 0 at time $t = 0$. Let $0 \leq x_i(t) < \infty$ denote the distance traveled by the i^{th} vehicle with respect to a fixed reference point on the roadside (without loss of generality we assume that this reference point is the point 0), and $v_i(t)$, $a_i(t)$ denote the speed and acceleration at time $t \geq 0$, respectively. Moreover, let $y_i(t) = x_{i+1}(t) - x_i(t) - L$ be the relative spacing of the i^{th} vehicle with respect to the vehicle $i + 1$ ahead at time $t \geq 0$, where $x_{n+1} \equiv P + x_1$ due to the periodicity of the ring road. Throughout the paper, except when needed, we use x_i , v_i , a_i , and y_i without explicitly mentioning their dependence on time. For simplicity of notations, we formulate the vehicle model and controller design for an ego vehicle with subscript e and use the subscript l in order to differentiate between the ego vehicle and its vehicle ahead, i.e., the lead vehicle. Note that by definition, $\sum_{i=1}^n y_i = P - nL$. This constraint is the main contrast to a straight line with no space limitation. An illustration of this setup for three vehicles is depicted in Figure 1.

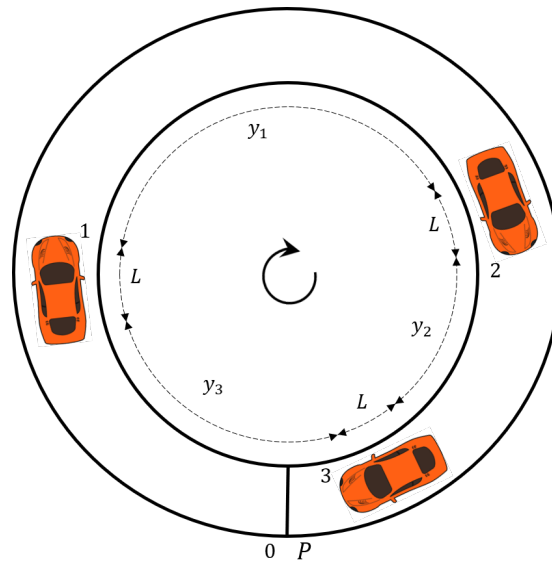


Figure 1: Example of three vehicles on a closed ring road setup

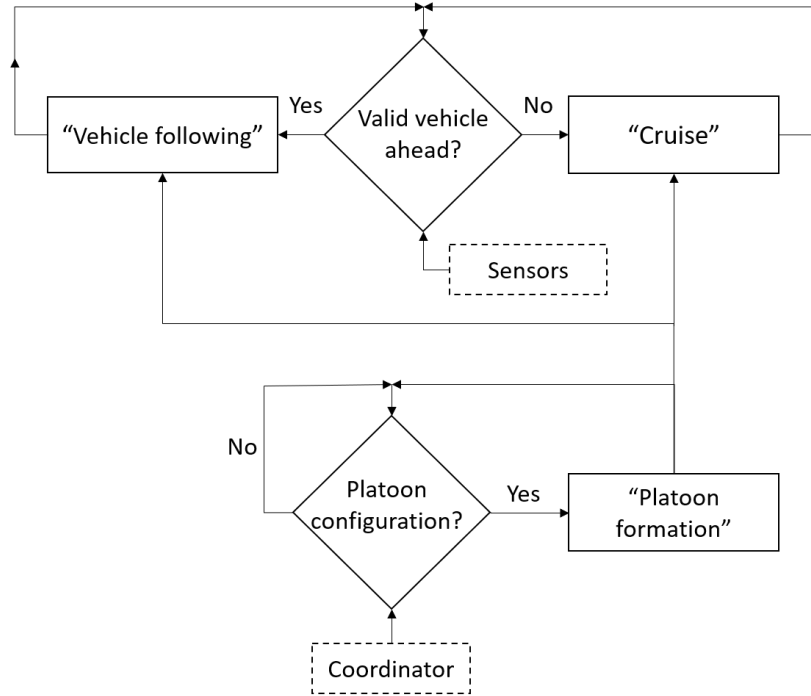


Figure 2: Logic diagram for determining the mode of operation

B. Modes of Operation

Each vehicle operates in one of the following two modes of operation: cruise control or vehicle following, see Figure 2. If there is no central coordination, an ego vehicle operates in the cruise mode if no valid vehicle is ahead that is within its sensing range. The validity of the lead vehicle is determined by comparing the relative spacing to a design threshold value. The ego vehicle is in the vehicle following mode, i.e., it follows the lead vehicle by keeping a safety distance, as long as the lead vehicle's speed is within the allowable speed limit. The speed limit is taken to be equal to the free flow speed V_f when there is no coordination. The platoon formation state in Figure 2 is activated in order to achieve a desired platoon formation when a central coordinator is present. This state will be discussed in detail in Section IV.

C. Vehicle Model

We assume that the road surface is horizontal and there is no wind gust. We use Newton's second law of motion for the ego vehicle to write,

$$m_e a_e = F_e - k_d v_e^2 - d_m(v_e)$$

where F_e is the engine force, m_e is the mass, k_d is the aerodynamic drag coefficient, and $d_m(v_e)$ is the mechanical friction of the ego vehicle travelling with the speed v_e [22]. Assuming a first-order engine dynamics we have,

$$\dot{F}_e = \frac{1}{\tau(v_e)}(\theta_e - F_e)$$

where θ_e is the throttle angle's force to the engine, and $\tau(v_e)$ is the engine's time constant at the speed v_e [23].

By combining the last two equations we derive,

$$\dot{a}_e = \beta(v_e, a_e) + \alpha(v_e)\theta_e$$

where,

$$\alpha(v_e) = \frac{1}{m_e \tau(v_e)}$$

$$\beta(v_e, a_e) = -2 \frac{k_d}{m_e} v_e a_e - \frac{1}{m_e} \dot{d}_m(v_e) - \frac{1}{\tau(v_e)} \left[a_e + \frac{k_d}{m_e} v_e^2 + \frac{d_m(v_e)}{m_e} \right]$$

At each speed v_e , throttle angle is chosen such that,

$$\theta_e = \frac{1}{\alpha(v_e)} [u_e - \beta(v_e, a_e)]$$

which leads to the equation,

$$\dot{a}_e = u_e \tag{1}$$

where u_e is to be designed to meet the control objectives presented below:

- 1) **Safety:** no rear-end collision under a worst-case stopping scenario as explained in [6]
- 2) **Smooth longitudinal maneuver:** Smooth position and/or speed tracking in the two modes of operation as well as a smooth transition between these modes
- 3) **String error attenuation:** attenuation of the amplitude of errors, e.g., in the position, upstream a platoon
- 4) **Passenger comfort:** $a_{min} \leq a_e \leq a_{max}$, except in an emergency braking scenario, and small jerk \dot{a}_e [5]

In the following sections, we design and analyze control laws that can meet the objectives with and without V2V communication and in the presence of a central coordinator.

III. VEHICLES ON A RING ROAD WITHOUT COORDINATION

A. No V2V Communication

In this section, we assume that vehicles do not communicate with each other and obtain the necessary data for cruising or vehicle following by using their own sensing capabilities. When the mode of operation is determined as explained in Section II-B, the sensing data are passed through appropriate filters [16] in order to generate continuous-time signals passed to the longitudinal controller u_e designed as follows:

- 1) **Cruise:**

$$u_e = K_a a_e + C_v(v_r - v_e) + \int_0^t [C_s(v_r - v_e)] d\tau \tag{2}$$

$$\dot{v}_r = \text{sat}[p(V_s - v_r)], \quad v_r(0) = v_e(0) \tag{3}$$

$$\text{sat}[x] = \begin{cases} a_{max} & \text{if } x \geq a_{max} \\ x & \text{if } a_{min} < x < a_{max} \\ a_{min} & \text{if } x \leq a_{min} \end{cases} \tag{4}$$

- 2) **Vehicle following:**

$$u_e = K_a a_e + C_p(t)\delta_e + C_v(v_r - v_e) + \int_0^t [C_q(\tau)\delta_e + C_s(v_r - v_e)] d\tau \tag{5}$$

$$v_r = v_l + (v_r(0) - v_l)e^{-\lambda t} \tag{6}$$

$$\delta_e = y_e - (h v_e + S_0) \tag{7}$$

where $K_a < 0$, $C_v, C_s, p, \lambda > 0$ are design constants, V_s is the speed limit and $V_s = V_f$. Moreover, the threshold distance Δ_d for switching from the cruise control mode to the vehicle following mode is chosen as follows,

$$\Delta_d = \begin{cases} hv_e + S_0 + r(v_e - v_l) & \text{if } v_e \geq v_l \\ hv_e + S_0 & \text{otherwise} \end{cases} \quad (8)$$

where $r > 0$ is a design constant. If the relative spacing of the ego vehicle with respect to the lead vehicle ahead is greater than Δ_d at $t = 0$, the ego vehicle starts operating in the cruise control mode and the speed tracking controller (2) is used. The reference speed v_r in this case is generated by passing the desired speed limit V_s through the nonlinear acceleration limiter filter (3) with the saturation function described in (4). The acceleration limiter prevents the acceleration outside the comfortable range when there is a large initial speed error $V_s - v_e(0)$ [5]. If the relative spacing becomes less than Δ_d at some time $t_0 \geq 0$, the ego vehicle switches to the vehicle following mode and the speed/position tracking controller (5) is used. The design parameters $C_p(t), C_q(t)$ are smoothly increased from zero to some positive design constants $C_p, C_q > 0$, i.e., $C_p(t) = C_p(1 - e^{-\lambda(t-t_0)})$, $C_q(t) = C_q(1 - e^{-\lambda(t-t_0)})$, $t \geq t_0$. Moreover, the reference speed v_r is smoothly changed from the initial value to the speed of the lead vehicle v_l (see (6)), and the reference relative spacing is set to $hv_e + S_0$ (see (7)), where $S_0 > 0$ is a constant standstill separation distance and h is a safe time headway constant. This is a well-known safe vehicle following strategy where the following vehicles try to keep a safe constant time headway from the vehicle ahead [6]. It was shown that the value of the time headway constant can be chosen such that two consecutive vehicles do not collide under a worst-case stopping scenario as explained in [6]. Accordingly, the switching distance Δ_d is chosen to be equal to the safety distance $hv_e + S_0$ plus an additional non-negative term $r(v_e - v_l)$ if the ego vehicle is travelling at least as fast as the lead vehicle (see (8)). The ego vehicle keeps operating in the vehicle following mode as long as the lead vehicle's speed is within its allowable speed limit V_s .

Remark 1. The objective is to design the control parameters such that (2) - (8) ensures stability, string error attenuation, and, lastly, satisfies comfort. We should emphasise that the designed longitudinal controller is only responsible for smoothly adjusting the spacing and/or speed. Other operations such as emergency braking are assessed by a higher-level supervisory controller and operated by different control laws which are not addressed in this paper. However, this problem is resolved in other papers, see for example [5], [16].

We define $n_c = \frac{P}{hV_f + S_0 + L}$ as the *critical number of vehicles* on the ring road (n_c can be non-integer). We also define *configuration* as the vector of relative spacings on the ring road.

Theorem 1. *There exist design parameters such that the following hold,*

- (i) *The controller (2) - (8) guarantees smooth vehicle following and/or speed tracking in all modes of operation and attenuation of the amplitude of errors with respect to the desired relative spacing, speed, and acceleration upstream a platoon.*
- (ii) *If $n < n_c$, there is an infinite number of vehicle configurations on the ring road; however the equilibrium speed is V_f in each of these configurations.*
- (iii) *If $n \geq n_c$, there is a unique vehicle configuration where all vehicles are symmetrically distributed around the ring road and their speed converges to an equilibrium speed of $\frac{1}{h}(\frac{P}{n} - S_0 - L) \leq V_f$.*

Proof. Refer to Appendix A. □

Remark 2. Equations (21), (29) in the proof of Theorem 1 suggest that when in the cruise control mode, a vehicle satisfies the comfortable acceleration limits and when in the vehicle following mode, it accelerates/decelerates at most as high as the vehicle ahead except, maybe, for an exponentially vanishing term. We confirm via simulations that this guarantees the specified comfort requirements except, maybe, for an exponentially vanishing time.

Remark 3. According to Theorem 1, for a given number of vehicles $n < n_c$, vehicles can form platoons of (possibly) different sizes with different inter-platoon spacing at steady state, which depends on the initial condition. We discuss in Section IV the role of central coordination in achieving a unique desired configuration in order to improve efficiency in utilizing the limited space.

Remark 4. Macroscopic traffic flow interpretation of Theorem 1: Let v^* be the equilibrium speed of vehicles, $\rho = \frac{n}{P}$ be the space-mean density, $\rho_c = \frac{n_c}{P}$ be the *critical density*, and $q^* = \rho v^*$ be the equilibrium space-mean flow. It follows from Theorem 1 that $v^* = \min\{V_f, \frac{1}{h}(\frac{P}{n} - S_0 - L)\}$. Therefore,

$$q^* = \begin{cases} V_f \rho & \text{if } \rho < \rho_c \\ \frac{1}{h}(1 - \rho(S_0 + L)) & \text{if } \rho \geq \rho_c \end{cases}$$

In other words, when the density is less than the critical density, the flow increases linearly with increasing density. However, when the density exceeds the critical density, the flow decreases linearly with increasing density. This gives rise to the well-known triangular fundamental diagram (see Figure 3). The maximum value of q^* , i.e., the *capacity* C of the ring road, is then found to be $C = \frac{V_f}{hV_f + S_0 + L}$.

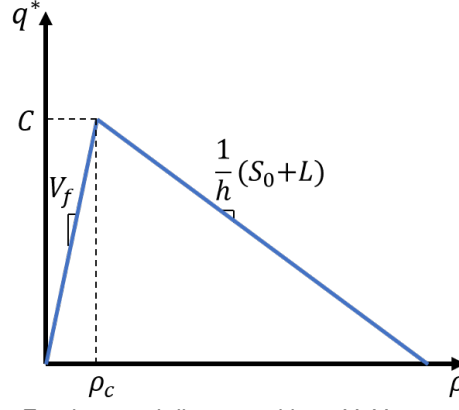


Figure 3: Fundamental diagram without V2V communication

Remark 5. According to the proof of Theorem 1, for speed tracking in the cruise control mode the poles of $K(s)$ in (19) must lie in the open left half of the s -plane. This condition is satisfied if,

$$K_a C_v + C_s < 0 \quad (9)$$

Moreover, for position/speed tracking and string error attenuation in the vehicle following mode, the design parameters must be chosen such that poles of $G(s)$ in (27) have negative real parts and $|G(j\omega)| \leq 1, \forall \omega \geq 0$. The former can be guaranteed by using pole placement. Additionally, $|G(j\omega)| \leq 1, \forall \omega \geq 0$ is satisfied if,

$$\begin{aligned} C_1 &\geq 0 \\ C_2 - C_v^2 &\geq 0 \end{aligned} \quad (10)$$

where,

$$\begin{aligned} C_1 &= K_a^2 - 2(hC_p + C_v) \\ C_2 &= (hC_p + C_v)^2 + 2C_q + 2K_a(C_p + hC_q + C_s) \end{aligned}$$

We provide a set of parameters in Section V that satisfies (9) and (10) (refer to (14)) as well as the stability criterion for $G(s)$.

B. V2V Communication

We now assume that vehicles are able to communicate their braking capabilities as well as their instantaneous acceleration and deceleration to their immediate predecessor. This feature allows for accurate reference tracking when vehicles are outside the sensing range and also smaller safe time headway constant between vehicles [24]. With V2V communication, the longitudinal control law in the vehicle following mode (5) is modified as follows,

$$\begin{aligned} u_e &= K_a a_e + C_p(t)\delta_e + C_v(v_r - v_e) + C_a(t)(a_l - a_e) \\ &+ \int_0^t [C_q(\tau)\delta_e + C_s(v_r - v_e) + C_b(\tau)(a_l - a_e)]d\tau \end{aligned} \quad (11)$$

where $C_a(t), C_b(t) \geq 0$ are additional control parameters which behave similar to $C_p(t), C_q(t)$. Note that the only difference between (5) and (11) is the additional acceleration terms $C_a(t)(a_l - a_e)$ and $C_b(t)(a_l - a_e)$ in (11). Since by choosing $C_a(t) = C_b(t) = 0, \forall t \geq 0$, (11) becomes identical to the control law in (5) all of the results for stability, string error attenuation, and comfort holds when V2V communication is possible. In fact, V2V communication adds additional degrees of freedom in choosing the design constants in order to guarantee good tracking performance.

As mentioned earlier, V2V communication reduces the minimum safe time headway constant h . Thus, the critical number of vehicle n_c for which vehicles can operate at the free flow speed increases. As a result, the critical density $\rho_c = \frac{1}{hV_f + S_0 + L}$ and the capacity $C = \frac{V_f}{hV_f + S_0 + L}$ in Remark 4 are increased. Therefore, V2V communication expands the free-flow region of the Fundamental diagram, see Figure 4.

Furthermore, using V2V communication, vehicles can be organized in platoons and decide among themselves certain configurations. Moreover, it allows for accurate tracking of the position, speed, and acceleration of vehicles ahead even when they are outside the sensing range. This feature expands the number of possible configurations that can be achieved in the presence of a coordinator. We discuss this in the next section.

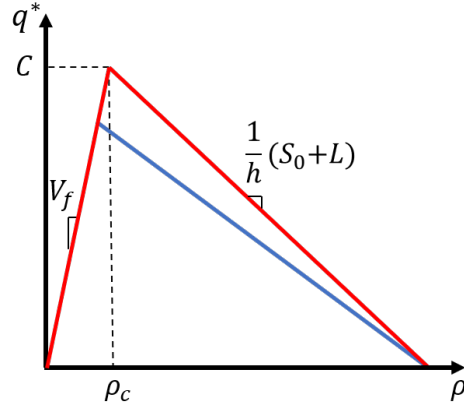


Figure 4: Fundamental diagrams with V2V communication (red) and without V2V communication (blue)

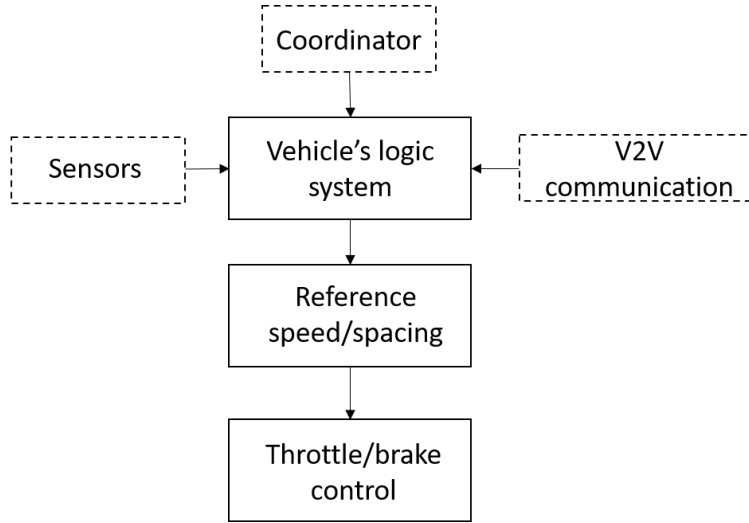


Figure 5: Control structure in the presence of a coordinator and/or V2V communication

IV. COORDINATION OF VEHICLES ON A RING ROAD

In the previous section, we assumed that vehicles travel without coordination, i.e., their action to achieve the speed limit or follow a vehicle in front was determined by their own sensors and/or V2V communication. According to Theorem 1, if $n < n_c$, there is an infinite number of configurations in which the system of vehicles can occupy the limited space but, in all of them, they travel with the free flow speed V_f . It may so happen that some configurations on the road are more desirable than others from the point of view of a central coordinator. For example, vehicles may be organized in closed-space platoons in order to decrease air drag and thus fuel consumption, or use the bandwidth of the coordinator-to-vehicle communication system more effectively by only communicating to the leaders of platoons [16].

In this section, we assume that vehicles use their own sensors and/or V2V communication in combination with commands from a central coordinator, see Figure 5. The coordinator chooses a configuration from the following set of desired configurations and communicates it along with the perimeter of the road P , and the number of vehicles n to certain vehicles:

- 1) **1-platoon asymmetrical**: a single platoon of n vehicles
- 2) **Symmetrical**: all vehicles sharing the limited space equally
- 3) **m -platoon symmetrical**: m platoons of vehicles, $1 < m \leq \frac{n}{2}$, sharing the limited space equally

These configurations are chosen in order to illustrate the idea. The following discussion can be easily applied to other desired configurations as well. Upon receiving commands from the coordinator, the ego vehicle calculates the appropriate reference speed and spacing according to the desired configuration and passes it to the longitudinal controllers u_e in (2), (5) with the

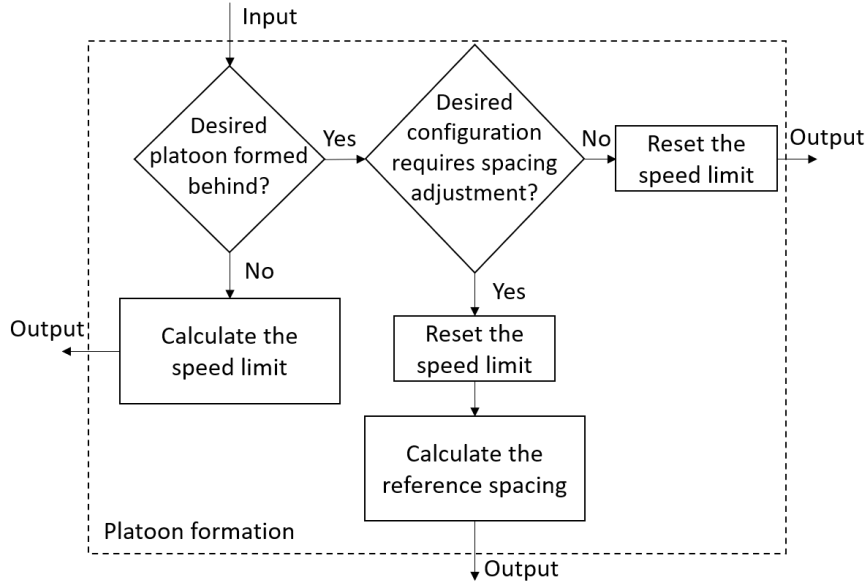


Figure 6: Logic diagram of a desired leader for creating the desired platoon

reference speed and spacing modified as follows,

$$V_s = \begin{cases} V_f & \text{if desired platoon formed behind} \\ \alpha V_f & \text{otherwise} \end{cases} \quad (12)$$

$$\delta_e = y_e - y_d$$

$$y_d = \begin{cases} (h_d + (h - h_d)e^{-\lambda t})v_e + S_0 & \text{if desired configuration requires} \\ h v_e + S_0 & \text{spacing adjustment} \\ h v_e + S_0 & \text{otherwise} \end{cases} \quad (13)$$

Upon receiving initiation commands from the coordinator at $t = 0$, the ego vehicle uses the platoon formation flow chart in Figure 6 in order to calculate the reference speed and spacing. According to Figure 6, when the platoon for which the ego vehicle is its desired leader has not yet formed, the ego vehicle changes its speed limit V_s from V_f to αV_f for some $\alpha \in (0, 1)$ (see (12)). According to the switching logic explained in Section II-B, it starts to decelerate, when it is safe, so that the vehicles behind catch up. When the desired platoon has formed, the ego vehicle is notified by the coordinator and/or V2V communication and the speed limit is reset to V_f (see (12)). Moreover, if the ego vehicle needs to adjust its relative spacing depending on the desired configuration, the controller smoothly tracks v_l and changes the reference relative spacing from the initial value to $h_d v_e + S_0$ (see (13)). The reference time headway constant h_d is calculated by the ego vehicle such that $h_d V_f + S_0$ is equal to the reference relative spacing, e.g., when the desired configuration is symmetrical, the reference relative spacing is $\frac{P}{n} - L$, and $h_d = \frac{1}{V_f}(\frac{P}{n} - L - S_0)$. Since the reference time headway constant h_d is different than h , the design parameters $C_p(t), C_q(t)$ in (2) are also smoothly changed, if necessary, such that the controller maintains good tracking performance.

As an example, consider the 1-platoon asymmetrical desired configuration and let the ego vehicle be its desired leader. Then, if the desired platoon has not yet formed, the ego vehicle switches to the cruise control mode, when it is safe, in order to track the reference speed of αV_f , $\alpha \in (0, 1)$, until all other vehicles catch up and switch to the vehicle following mode. At this point, it starts tracking the reference free flow speed V_f and the transition is completed.

Note that in Section III, vehicles used homogeneous time headway constants h , and constant desired speed V_f in the cruise control mode. However, with the coordinator in the loop the desired time headways are (possibly) heterogeneous and time-varying, and the reference speed in the cruise control mode is, in general, piece-wise constant. Therefore, additional analysis is required in order to establish stability.

Theorem 2. *There exist design parameters such that the longitudinal controller (2)-(8) with the reference speed/spacing specified in (12), (13), guarantees that the system of vehicles converges to the configuration specified by the coordinator.*

Proof. Refer to Appendix B. □

Remark 6. Consider the m -platoon symmetrical desired configuration, $1 < m \leq \frac{n}{2}$. Then, the equilibrium distance between adjacent platoons is $d = \frac{n}{m}(\frac{P}{n} - L - h V_f - S_0) + h V_f + S_0$. Since $P > n(L + h V_f + S_0)$, i.e., $n < n_c$, d decreases when m

is increased from 2 to $\frac{n}{2}$. In other words, as the size of the platoon increases in the m -platoon symmetrical configuration, the desired inter-platoon relative spacing increases. Since the sensing range of vehicles are limited, V2V communication allows accurate tracking of the position of the vehicle ahead even when it is outside of the sensing range. In other words, V2V communication expands the number of achievable desired configurations when there is central coordination.

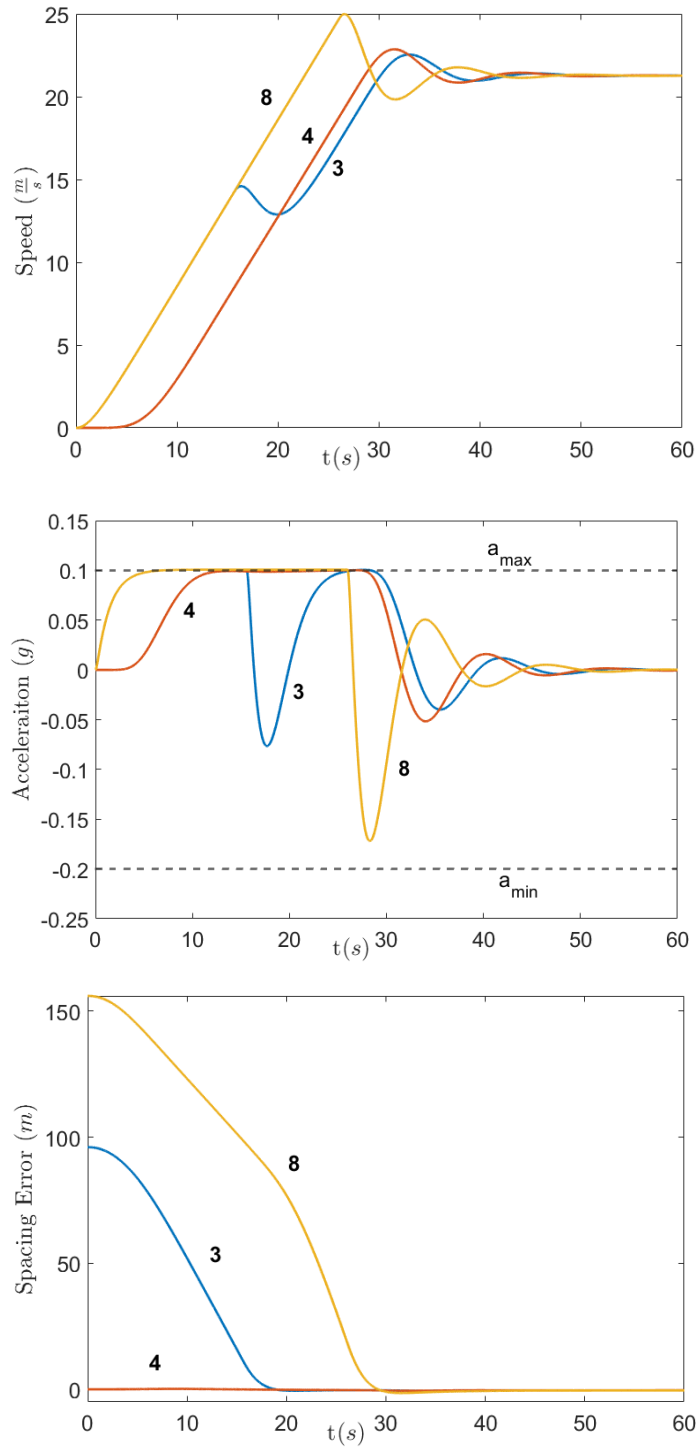


Figure 7: Simulation results for the high density traffic regime

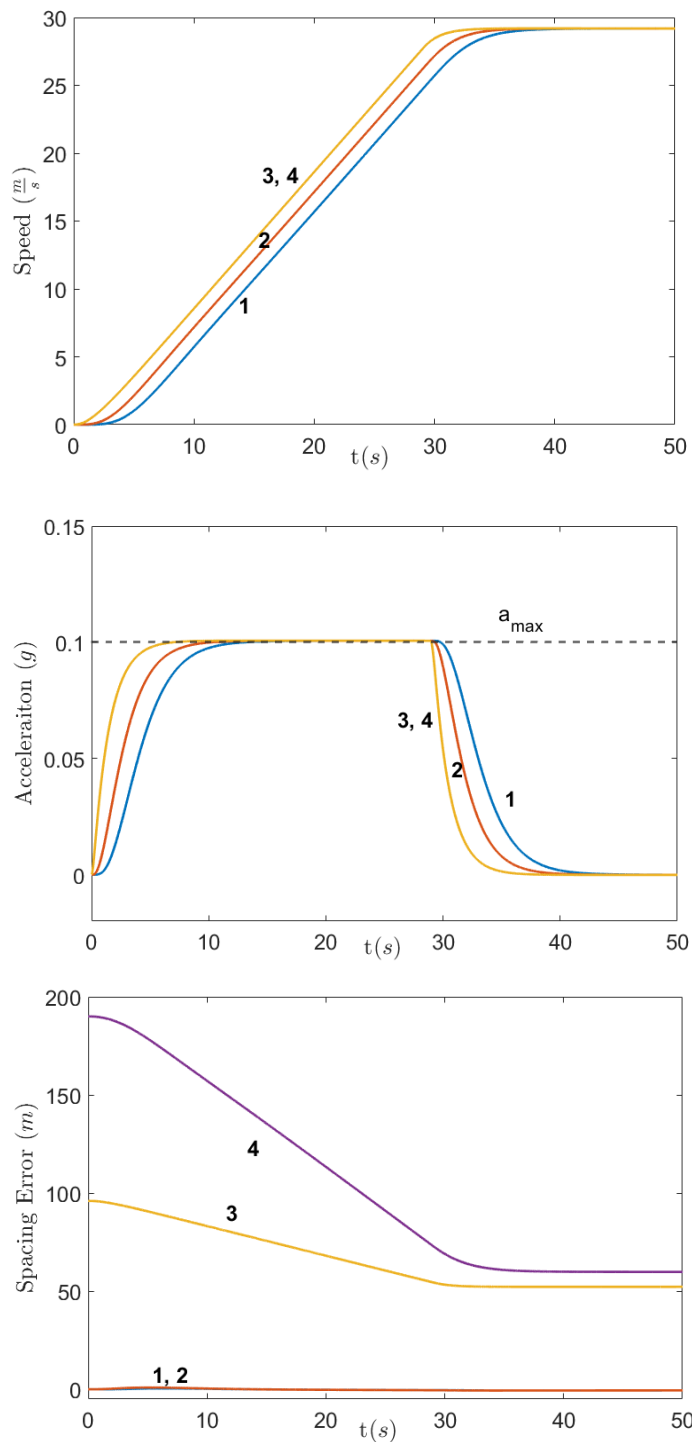


Figure 8: Simulation results for the low density traffic regime with no coordination

V. SIMULATION RESULTS

In this section, we illustrate the performance of the designed control laws by simulating a few scenarios. In all scenarios, the control parameters are chosen as follows,

$$\begin{aligned}
 K_a &= -9, \quad C_p = 2, \quad C_v = 6, \quad C_q = 0.01, \quad C_s = 0.03 \\
 h &= 1.5 \text{ [s]}, \quad S_0 = 4 \text{ [m]}, \quad p = 10, \quad a_{min} = -0.2g \\
 a_{max} &= 0.1g, \quad r = 1, \quad \lambda = 0.5
 \end{aligned} \tag{14}$$

For this choice of design constants, it can be checked that stability, string error attenuation, and comfort conditions are

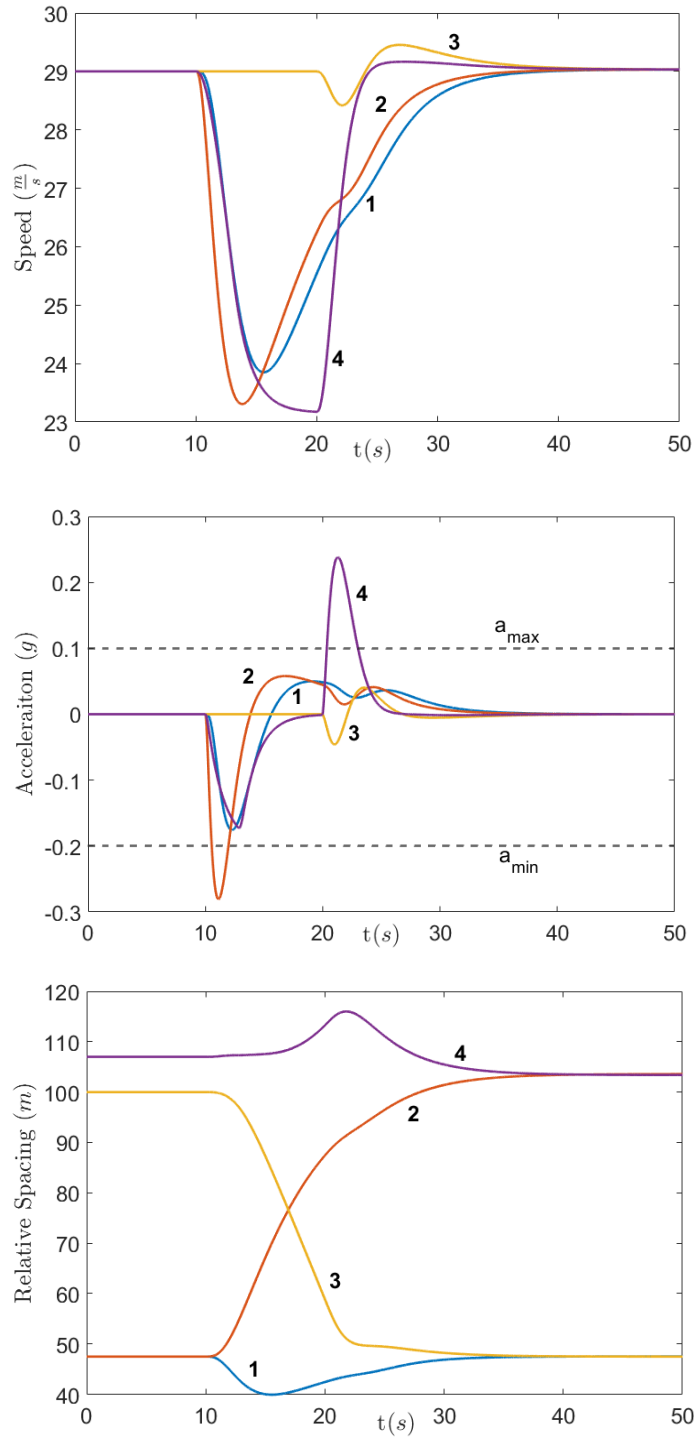


Figure 9: Simulation results with coordination and 2-platoon symmetrical desired configuration

satisfied. Other parameters are chosen to be as follows,

$$P = 320 [m], \quad L = 4.5 [m], \quad V_f = 29 \left[\frac{m}{s}\right]$$

Therefore, the critical number of vehicles is $n_c = \frac{320}{1.5 \times 29 + 4 + 4.5} = 6.04$.

A. High Density Traffic Regime

Let $n = 8 > n_c$, i.e., a high-density traffic regime, with two platoons of sizes 3 and 5 initially at rest. The first platoon consists of vehicles 1 – 3 with vehicle 3 as the leader, and the second platoon consists of vehicles 4 – 8 with vehicle 8 as the

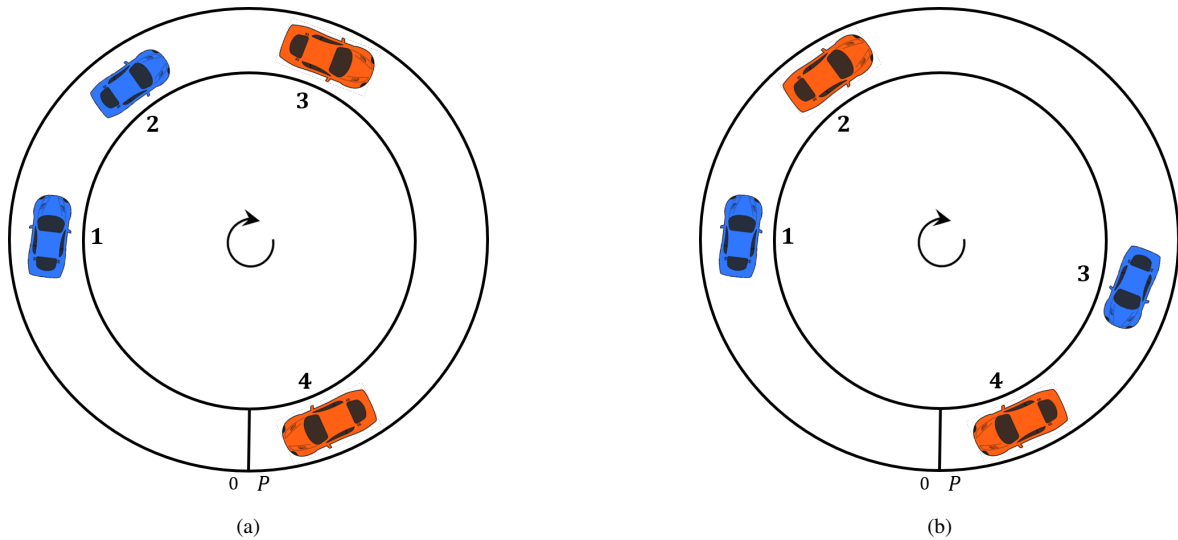


Figure 10: Steady state configuration of vehicles when there is (a) no coordination, (b) coordination with 2-platoon symmetrical desired configuration, where vehicles in the cruise control mode are colored in orange and the ones in the vehicle following are colored blue

leader. The distance between the first and second platoons is initially 100 meters, i.e., $y_3(0) = 100$ [m], and all the following vehicles are assumed to be at the desired spacing at $t = 0$. According to Theorem 1, the system of vehicles converges to a unique configuration with the equilibrium relative spacing of $\frac{P}{n} - L = 35.5$ [m], and speed of $\frac{1}{h}(\frac{P}{n} - S_0 - L) = 21$ [$\frac{m}{s}$]. The speed, acceleration, and spacing error profiles for sample vehicles are shown in Figures 7. As can be seen from the acceleration and speed profiles, the leader of the first platoon, i.e., vehicle 3, operates in the cruise control mode until $t \approx 15$ [s]. At this point it switches to the vehicle following mode and the two platoons become connected. Furthermore, the leader of the second platoon switches to the vehicle following mode at $t \approx 26$ [s], and a platoon with no leader is formed. It is clear that the speed and acceleration profiles are smooth and within the comfort range in both modes of operation as well as during the transition between the two modes.

B. Low Density Traffic Regime: No Coordination

In this scenario, let $n = 4 < n_c$, i.e., a low-density traffic regime, and all vehicles are initially at rest. We assume that vehicles 1 – 3 are initially in platoon formation with the following vehicles at desired spacing, and vehicle 4 is 100 meters ahead. The speed, acceleration, and spacing error profiles of the vehicles are shown in Figure 8. It can be seen from the spacing error profiles that vehicles 3 and 4 operate in the cruise control mode at all times, thus at steady state, we have one platoon of three vehicles with vehicle 3 as the leader, and a single vehicle, i.e., vehicle 4, operating in the cruise control mode, see Figure 10a. Moreover, it can be easily verified that all vehicles reach the free flow speed V_f while satisfying the the acceleration bounds during the transient. Also, it can be seen from the acceleration profiles that the errors in acceleration are not magnified upstream a platoon, i.e., string error attenuation.

C. Low Density Traffic Regime: With Coordination

We again consider $n = 4$. We assume that vehicles are travelling at steady state speed of V_f and initial configuration of the previous scenario. Let the coordinator's desired configuration be 2-platoon symmetrical with vehicles 2 and 4 as the desired leaders. The simulation results for this scenario are shown in Figure 9. The coordinator communicates the desired configuration to vehicles 2 and 4 at $t = 10$ [s]. Since the platoon consisting of vehicles 3 and 4 has not formed at $t = 10$ [s], vehicle 4 sets its speed limit to $V_s = 0.8V_f$, and starts to decelerate until vehicle 3 catches up. At the same time vehicle 2 smoothly increases its time headway constant to the desired value $h_d \approx 3.43$ [s], and starts decelerating in order to adjust its relative spacing. At $t \approx 20$ [s], vehicle 3 switches to the vehicle following mode, and vehicle 4 resets its speed limit while smoothly increasing its desired relative spacing to $h_d v_1 + S_0$. Due to large initial positive relative spacing and speed error at $t \approx 20$ [s], this introduces acceleration outside the comfortable bounds for vehicle 4. It can be seen from the relative spacing profiles at $t \approx 35$ [s], that the desired configuration is achieved asymptotically. The qualitative steady state configuration of this scenario is shown in Figure 10b.

VI. CONCLUSION

In this paper we considered the design of vehicle longitudinal controllers for homogeneous vehicles following a single lane in a closed ring road under safety and comfort constraints in order to evaluate the impact of limited space on the speed of flow.

We showed that if the number of vehicles is less than a certain critical number n_c , which depends on the perimeter of the ring road, free flow speed limit, and safety spacing, the vehicles can organize themselves around the ring road in an infinite number of different configurations. When the number of vehicles increases to be greater than or equal to n_c , all vehicles converge to a unique equilibrium configuration where the equilibrium speed decreases as the number of vehicles increases. When we add vehicle to vehicle communications, the controller is modified for faster action during vehicle following and safety can be guaranteed under lower intervehicle spacing. As a result, the critical number of vehicles n_c that can operate at the maximum allowable speed increases. We also show that if a central coordinator dictates the configuration of the vehicles around the ring road, the proposed controllers can force the vehicles to converge to the desired coordination while respecting the safety and passenger comfort constraints. Computer simulations are used to demonstrate the performance of the controllers.

APPENDIX A
PROOF OF THEOREM 1

- (i) Let $w_e = \int_0^t [C_q(\tau)\delta_e + C_s(v_r - v_e)]d\tau$, where $C_q(t) = 0$ when the ego vehicle is in the cruise control mode. We consider the following three cases. First, let the ego vehicle be operating in the cruise control mode. The closed loop dynamics of the ego vehicle can be written as follows,

$$\begin{aligned}\dot{v}_e &= a_e \\ \dot{a}_e &= K_a a_e + C_v(v_r - v_e) + w_e \\ \dot{w}_e &= C_s(v_r - v_e) \\ \dot{v}_r &= \text{sat}[p(V_f - v_r)]\end{aligned}\tag{15}$$

In an equilibrium point of (15) we have,

$$\begin{aligned}a_e &= 0 \\ C_v(v_r - v_e) + w_e &= 0 \\ C_s(v_r - v_e) &= 0 \\ v_r &= V_f\end{aligned}\tag{16}$$

and $(v_e, a_e, w_e, v_r) = (V_f, 0, 0, V_f)$ is the unique equilibrium of this mode. Without loss of generality, suppose that $p(V_f - v_r(0)) > a_{max}$, i.e., the saturation function is initially active. It follows that,

$$v_r(t) = \begin{cases} a_{max}t & \text{if } 0 \leq t \leq T \\ -\frac{a_{max}}{p}e^{-p(t-T)} + V_f & \text{if } T \leq t \end{cases}\tag{17}$$

where $T = \frac{V_f}{a_{max}} - \frac{1}{p}$. Hence, $v_r \rightarrow V_f$ exponentially fast as $t \rightarrow \infty$. As a result, the state of the saturation function converges to its linear region and (15) becomes a LTI system after a finite time. By shifting the equilibrium point of (15) to zero and taking Laplace transform of the first three equations assuming zero initial condition, it follows that,

$$V_e(s) = K(s)V_r(s)\tag{18}$$

where $V_e(s), V_r(s)$ are Laplace transforms of v_e, v_r , respectively, and,

$$K(s) = \frac{C_v s + C_s}{s^3 - K_a s^2 + C_v s + C_s}\tag{19}$$

For stability of the equilibrium, we require that poles of $K(s)$ lie in the open left half of the complex plane. For analyzing the performance in achieving comfort, note that from (18) we obtain,

$$A_e(s) = sK(s)V_r(s)\tag{20}$$

where $A_e(s)$ is the Laplace transform of a_e . Therefore, if we choose the design constants such that $|K(j\omega)| \leq 1, \forall \omega \geq 0$ and $k(t) \geq 0, \forall t \geq 0$, then $\|k(t)\|_1 \leq 1$. Thus, assuming zero initial condition, it follows from (17) and (20) that for all $t \geq 0$,

$$|a_e(t)| \leq \|k(t)\|_1 \sup_{t \geq 0} |\dot{v}_r(t)| \leq a_{max}\tag{21}$$

Similarly, if the saturation function is initially active in the other direction, i.e., $p(V_f - v_r(0)) < a_{min}$, then $a_e(t) \geq a_{min}$. Next, let the ego vehicle switch to the vehicle following mode at time $t = 0$. The closed loop dynamics of the ego vehicle can be written as follows,

$$\begin{aligned}\dot{y}_e &= v_l - v_e \\ \dot{v}_e &= a_e \\ \dot{a}_e &= K_a a_e + C_p(t)\delta_e + C_v(v_l + (v_r(0) - v_l)e^{-\lambda t} - v_e) + w_e \\ \dot{w}_e &= C_q(t)\delta_e + C_s(v_l + (v_r(0) - v_l)e^{-\lambda t} - v_e)\end{aligned}\tag{22}$$

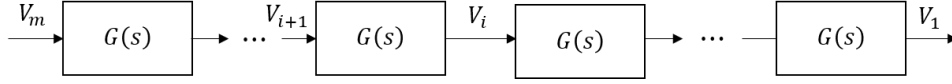
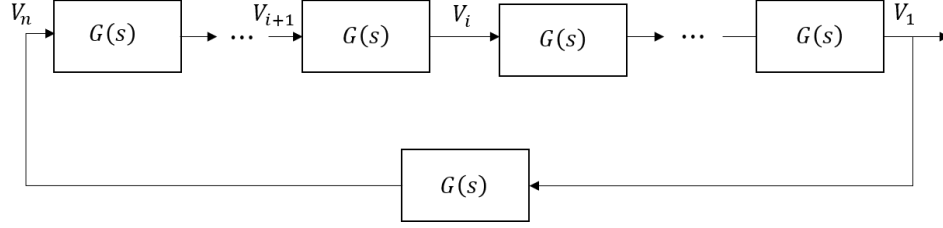
Figure 11: Block diagram of a platoon of m vehicles with vehicle m as the leader

Figure 12: Block diagram of a platoon with no leader

Assuming constant v_l and neglecting the exponentially vanishing terms, the equilibrium point of (22) is,

$$\begin{aligned} v_e &= v_l \\ a_e &= 0 \\ C_p(t)(y_e - hv_e - S_0) + C_v(v_l - v_e) + w_e &= 0 \\ C_q(t)(y_e - hv_e - S_0) + C_s(v_l - v_e) &= 0 \end{aligned} \quad (23)$$

Therefore, $(y_e, v_e, a_e, w_e) = (hv_e + S_0, v_l, 0, 0)$ is the unique equilibrium of (22). Let $z_e^T = (y_e \ v_e \ a_e \ w_e)$. Note that since $v_r(0)e^{-\lambda t} \rightarrow 0$ exponentially fast as $t \rightarrow \infty$, it has no effect on the stability and is ignored in the analysis that follows. By shifting the equilibrium to zero, (22) can be written in the following compact form,

$$\dot{z}_e = (A_1 + D_1(t))z_e + (B_1 + D_2(t))v_l \quad (24)$$

where,

$$\begin{aligned} A_1 &= \begin{pmatrix} 0 & -1 & 0 & 0 \\ 0 & 0 & 1 & 0 \\ C_p & -(hC_p + C_v) & K_a & 1 \\ C_q & -(hC_q + C_s) & 0 & 0 \end{pmatrix}, \quad B_1 = \begin{pmatrix} 1 \\ 0 \\ C_v \\ C_s \end{pmatrix}, \\ D_1(t) &= \begin{pmatrix} 0 & 0 & 0 & 0 \\ 0 & 0 & 0 & 0 \\ -C_p e^{-\lambda t} & C_p h e^{-\lambda t} & 0 & 0 \\ -C_q e^{-\lambda t} & C_q h e^{-\lambda t} & 0 & 0 \end{pmatrix}, \quad D_2(t) = \begin{pmatrix} 0 \\ 0 \\ -C_v e^{-\lambda t} \\ -C_s e^{-\lambda t} \end{pmatrix} \end{aligned} \quad (25)$$

Since $D_1(t), D_2(t) \rightarrow 0$ as $t \rightarrow \infty$, the equilibrium of (24) is exponentially stable if the equilibrium of the LTI system $\dot{z}_e = A_1 z_e + B_1 v_l$ is exponentially stable [25]. By taking Laplace transform of the corresponding LTI system, we arrive at the following relationship,

$$V_e(s) = G(s)V_l(s) + E_0(s) \quad (26)$$

where $E_0(s)$ is due to non-zero initial condition of the ego vehicle and,

$$\begin{aligned} G(s) &= \frac{C_v s^2 + (C_p + C_s)s + C_q}{F(s)} \\ F(s) &= s^4 - K_a s^3 + (hC_p + C_v)s^2 + (C_p + hC_q + C_s)s + C_q \end{aligned} \quad (27)$$

We consider two possible cases. In the first case, the ego vehicle has joined a platoon of m vehicles, $m \in \mathcal{N}$, with the leader in the cruise control mode, see Figure 11. In this case, the stability of the equilibrium is guaranteed if poles of $G(s)$ lie in the open left half of the s -plane. In the second case, the ego vehicle has joined a platoon with no leader, see Figure 12. It is well-known [25] that a sufficient condition for exponential stability of the equilibrium of the system in Figure 12 is that poles of $G(s)$ lie in the open left half of the s -plane and $|G(j\omega)| \leq 1, \forall \omega \geq 0$.

For analyzing the performance of the controller in achieving passenger comfort, we assume that $C_p(t), C_q(t)$ are constant and $v_r = v_l$ in the vehicle following mode in order to make use of the properties of LTI systems. However, we demonstrate by simulations that the proposed controller achieves smooth and comfortable acceleration during transient even if these assumptions do not hold. It follows from (26) that,

$$A_e(s) = G(s)A_l(s) + \tilde{E}_0(s) \quad (28)$$

where $G(s)$ is specified in (27) and $\tilde{E}_0(s) = sE_0(s) + G(s)v_l(0) - v_e(0)$ is due to non-zero initial condition. Since $|G(j\omega)| \leq 1, \forall \omega \geq 0$ in order to guarantee stability, if we choose the design constants such that $g(t) \geq 0, \forall t \geq 0$, we have,

$$|a_e(t)| \leq |a_l(t)| + \tilde{e}_0(t) \quad (29)$$

where $\tilde{e}_0(t)$ is the inverse Laplace transform of $\tilde{E}_0(s)$ and is exponentially vanishing. Thus, the the following vehicles accelerate/decelerate at most as high as the vehicle ahead except, maybe, for an exponentially vanishing term.

We now analyze the attenuation of errors in, e.g., the position, of a vehicle upstream the platoon. Consider a platoon of m vehicles, $m \in \mathcal{N}$, travelling with a constant speed such that for $i = 1, 2, \dots, m-1, \delta_i(0) = 0$. Assume that there is a small perturbation in the position of the lead vehicle, i.e. vehicle m . Since we are assuming a small perturbation, we can neglect the dynamics of the acceleration limiter filter. By assuming $C_p(t) = C_p, C_q(t) = C_q, v_r = v_l$, for all of the following vehicles and taking Laplace transform of the equations in (22) we obtain,

$$\frac{\Delta_i}{\Delta_{i+1}}(s) = G(s), \quad i = 1, 2, \dots, m-2 \quad (30)$$

where $\Delta_i(s), \Delta_{i+1}(s)$ are the Laplace transforms of δ_i, δ_{i+1} , respectively, and $G(s)$ is given in (27). The necessary and sufficient condition for string error attenuation in the \mathcal{L}_2 sense is that $|G(j\omega)| \leq 1, \forall \omega \geq 0$ [6]. Note that this condition is already satisfied in order to ensure stability of the equilibrium. Moreover, a sufficient condition for string error attenuation in the \mathcal{L}_∞ sense is that $|G(j\omega)| \leq 1, \forall \omega \geq 0$, and $g(t) \geq 0, \forall t \geq 0$ [6]. This condition is also satisfied in order to provide comfort. Finally, due to homogeneity of vehicles, string error attenuation extends to the speed and acceleration errors (see also (26) and (28)).

- (ii) Let $n < n_c$, or equivalently $P > n(hV_f + S_0 + L)$. We claim that at least one vehicle must be operating in the cruise control mode at steady state. Suppose not; then from the equilibrium analysis in (23) it follows that at steady state we have for every $i \in \mathcal{N}$ that $y_i = hv_i + S_0, v_i = v_{i+1}$. Therefore, $y_i = hv_i + S_0 = hv_{i+1} + S_0 = y_{i+1}$. Since $\sum_{i=1}^n y_i = P - nL$, we obtain for every $i \in \mathcal{N}$ that $y_i = \frac{P}{n} - L$ and,

$$v_i = \frac{1}{h} \left(\frac{P}{n} - S_0 - L \right) > V_f$$

which cannot occur because, according to the designed logic, this violates the speed limit V_f . It follows from the equilibrium analysis in (16), (23) and the stability of the equilibrium from the previous part that for every $i \in \mathcal{N}$, if vehicle i operates in the cruise control mode at steady state, its speed converges to V_f . Moreover, it is required from the switching logic that $\delta_i \geq 0$. Hence, the relative spacing of vehicle i converges to $hV_f + S_i$, where $S_i \geq S_0$ depends on the initial condition. On the other hand, if vehicle i operates in the vehicle following mode, its speed converges to V_f , and its relative spacing converges to $hV_f + S_0$.

- (iii) Let $n \geq n_c$, or equivalently $P \leq n(hV_f + S_0 + L)$, then all vehicles must be operating in the vehicle following mode at steady state. Otherwise, using a similar argument as before we arrive at the contradiction $P > n(hV_f + S_0 + L)$. Hence, for every $i \in \mathcal{N}$, the relative spacing of vehicle i converges to $\frac{P}{n} - L$, and its speed converges to $\frac{1}{h} \left(\frac{P}{n} - S_0 - L \right)$.

APPENDIX B PROOF OF THEOREM 2

Since the constant term S_0 has no effect on the stability, we neglect it in the analysis whenever needed. We consider the following three cases: first, consider the 1-platoon asymmetrical desired configuration and let the ego vehicle be the desired leader. At $t = 0$, the ego vehicle sets its speed limit to $\alpha V_f, \alpha \in (0, 1)$, and starts tracking αV_f . Using the equilibrium equations in (16), it follows that the equilibrium of the closed loop dynamics of the ego vehicle is $v_e = v_r = \alpha V_f, a_e = 0$, and $w_e = 0$. Since at the equilibrium we must have $v_i = v_e = \alpha V_f, i \in \mathcal{N}$, and $\alpha < 1$, it follows that no other vehicle can be operating in the cruise control mode at steady state. Therefore, all of the vehicles switch to the vehicle following mode after a finite time and form a platoon of n vehicles with the ego vehicle as its leader. Using αV_f instead of V_f in the analysis from (17) - (26), exponential stability of the equilibrium of the platoon immediately follows. Similarly, the equilibrium state of the platoon is exponentially stable when the ego vehicle resets its speed limit to V_f . Note that the total number of switching in the reference speed and spacing is finite, thus the switching does not affect stability.

Consider the symmetrical desired configuration. Note that by construction, all vehicles eventually switch to the vehicle following mode in order to adjust their relative spacing by using the desired time headway constant and do not switch again at future times (see Figure 6). Thus, the switching does not affect the steady state behavior of vehicles. Without loss of generality, let the ego vehicle be in the vehicle following mode when it smoothly increases its time headway constant from h to h_1 at time $t = 0$, where h_1 is such that $h_1 V_f + S_0 = \frac{P}{n} - L$. The closed loop dynamics of the ego vehicle can be written as follows,

$$\begin{aligned} \dot{y}_e &= v_l - v_e \\ \dot{v}_e &= a_e \\ \dot{a}_e &= K_a a_e + C_p(t)(y_e - h(t)v_e) + C_v(v_l - v_e) + w_e \\ \dot{w}_e &= C_q(t)(y_e - h(t)v_e) + C_s(v_l - v_e) \end{aligned} \quad (31)$$

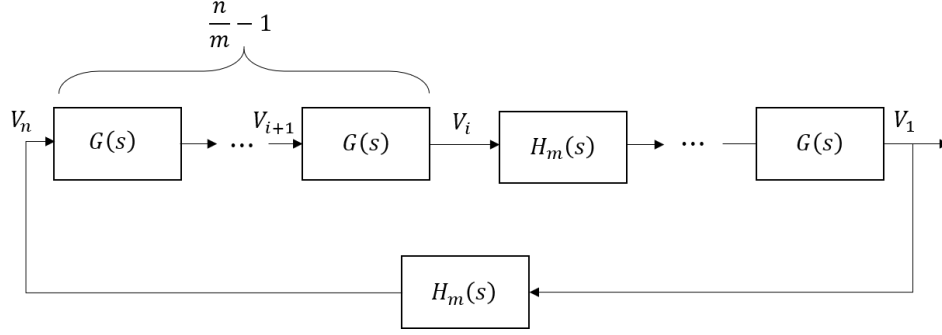


Figure 13: Block diagram of the m -platoon symmetrical configuration with vehicle n as the desired leader of a platoon

where $h(t) = h_1 + (h - h_1)e^{-\lambda t}$. The design parameters $C_p(t)$, $C_q(t)$ are also smoothly changed to desired values, e.g., $C_p(t) = \tilde{C}_p + (C_p - \tilde{C}_p)e^{-\lambda t}$, where $\tilde{C}_p > 0$ is a design constant to be chosen. Note that if the ego vehicle was operating in the cruise control mode at $t = 0$, its closed loop dynamics would have been the same as (31) except that $C_p(0) = C_q(0) = 0$, and $v_r = v_l + (v_r(0) - v_l)e^{-\lambda t}$. Let $z_e^T = (y_e \ v_e \ a_e \ w_e)$. We can write the closed loop dynamics (31) in the following compact form,

$$\dot{z}_e = (A_2 + D_3(t))z_e + B_2v_l \quad (32)$$

where,

$$A_2 = \begin{pmatrix} 0 & -1 & 0 & 0 \\ 0 & 0 & 1 & 0 \\ \tilde{C}_p & -(h_1\tilde{C}_p + C_v) & K_a & 1 \\ \tilde{C}_q & -(h_1\tilde{C}_q + C_s) & 0 & 0 \end{pmatrix}, \quad B_2 = \begin{pmatrix} 1 \\ 0 \\ C_v \\ C_s \end{pmatrix}$$

in which $D_3(t) \rightarrow 0$ exponentially fast as $t \rightarrow \infty$ and is not brought here for the sake of brevity. The equilibrium of (32) is exponentially stable if the equilibrium of the LTI system,

$$\dot{z}_e = A_2z_e + B_2v_l \quad (33)$$

is exponentially stable [25]. In order to find the stability condition, we use another representation of (33) by taking Laplace transform of both sides and deriving the following relationship,

$$V_e(s) = H_1(s)V_l(s) + E_0(s) \quad (34)$$

where $E_0(s)$ is due to non-zero initial condition of the ego vehicle and,

$$H_1(s) = \frac{\tilde{C}_ps + \tilde{C}_q}{s^4 - K_as^3 + (h_1\tilde{C}_p + C_v)s^2 + (\tilde{C}_p + h_1\tilde{C}_q + C_s)s + \tilde{C}_q}$$

is a transfer function similar to $G(s)$ in (27) only with different parameters. Since the desired configuration is symmetrical, i.e., $h_d = h_1$ for all vehicles, the closed loop dynamics of each vehicle on the ring road becomes the same as (31) after the final switching time only with (possibly) different initial values of the design parameters and reference speed. Hence, (34) holds for all vehicles in the corresponding LTI system and we have a similar block diagram as in Figure 12. Using a similar argument to the proof of Theorem 1, a sufficient condition for stability is that poles of $H_1(s)$ lie in the left half of the s -plane and $|H_1(j\omega)| \leq 1$, $\forall \omega \geq 0$. It can be verified that if the design constants K_a, C_p, C_q satisfy $K_aC_p + C_q < 0$, and \tilde{C}_p, \tilde{C}_q are chosen such that $h_1\tilde{C}_p = hC_p$, $h_1\tilde{C}_q = hC_q$, the stability conditions are guaranteed.

Finally, consider the m -platoon symmetrical desired configuration, $1 < m \leq \frac{n}{2}$, and let the ego vehicle be a desired leader. From the result for the 1-platoon asymmetrical configuration, it follows that after a finite time, all of the desired followers of the ego vehicle switch to the vehicle following mode. Also, similar to the symmetrical configuration, all vehicles eventually operate in the vehicle following mode and do not switch at future times. Assume that the ego vehicle sets its reference spacing to $h_mv_e + S_0$ at $t = 0$, where h_m is the desired time headway constant at the free flow speed calculated by the ego vehicle. The closed loop dynamics of the ego vehicle can be written as (31) with a different h_m and (possibly) different design constants and reference speed trajectory. Following a similar argument as in the previous scenario, the following relationship can be found for the corresponding LTI system,

$$V_e(s) = H_m(s)V_l(s) + E_0(s) \quad (35)$$

where $E_0(s)$ is due to non-zero initial condition and,

$$H_m(s) = \frac{\tilde{C}_ps + \tilde{C}_q}{s^4 - K_as^3 + (h_m\tilde{C}_p + C_v)s^2 + (\tilde{C}_p + h_m\tilde{C}_q + C_s)s + \tilde{C}_q}$$

where the constants \tilde{C}_p , \tilde{C}_q are to be chosen. Note that the Laplace domain relationship between the speeds of the following vehicles of a platoon is different than (35) and was derived in (26). Figure 13 shows the block diagram of this case after the final switching time. By using a similar argument as in the proof of Theorem 1, a sufficient condition for stability is that poles of $H_m(s)G(s)$ lie in the open left half of the s -plane, and $|H_m(j\omega)G(j\omega)| \leq 1$, $\forall \omega \geq 0$. Since the transfer function $G(s)$ is stable and satisfies $|G(j\omega)| \leq 1$, $\forall \omega \geq 0$, a sufficient condition for stability is that $H_m(s)$ is stable and $|H_m(j\omega)| \leq 1$, $\forall \omega \geq 0$. These conditions are automatically guaranteed if $K_a C_p + C_q < 0$, and $h_m \tilde{C}_p = h C_p$, $h_m \tilde{C}_q = h C_q$.

REFERENCES

- [1] D. Schrank, B. Eisele, T. Lomax, and J. Bak, "2015 urban mobility scorecard," 2015.
- [2] F. Alasiri, Y. Zhang, and P. A. Ioannou, "Robust variable speed limit control with respect to uncertainties," *European Journal of Control*, 2020.
- [3] P. Varaiya, "Smart cars on smart roads: problems of control," *IEEE Transactions on automatic control*, vol. 38, no. 2, pp. 195–207, 1993.
- [4] J. Rios-Torres and A. A. Malikopoulos, "A survey on the coordination of connected and automated vehicles at intersections and merging at highway on-ramps," *IEEE Transactions on Intelligent Transportation Systems*, vol. 18, pp. 1066–1077, May 2017.
- [5] P. Ioannou and Z. Xu, "Throttle and brake control systems for automatic vehicle following," *I V H S Journal*, vol. 1, no. 4, pp. 345–377, 1994.
- [6] P. Ioannou and C. Chien, "Autonomous intelligent cruise control," *IEEE Transactions On Vehicular Technology*, vol. 42, no. 4, pp. 657–672, 1993.
- [7] H. J. Swaroop D.D., "Constant spacing strategies for platooning in automated highway systems," *ASME. J. Dyn. Sys., Meas., Control*, vol. 121, no. 3, pp. 462–470, 1999.
- [8] E. Shaw and J. K. Hedrick, "String stability analysis for heterogeneous vehicle strings," in *2007 American Control Conference*, pp. 3118–3125, July 2007.
- [9] H. Tan, R. Rajamani, and W. Zhang, "Demonstration of an automated highway platoon system," in *Proceedings of the 1998 American Control Conference. ACC (IEEE Cat. No.98CH36207)*, vol. 3, pp. 1823–1827 vol.3, June 1998.
- [10] P. Seiler, A. Pant, and K. Hedrick, "Disturbance propagation in vehicle strings," *IEEE Transactions on Automatic Control*, vol. 49, pp. 1835–1842, Oct 2004.
- [11] P. Barooah, P. G. Mehta, and J. P. Hespanha, "Mistuning-based control design to improve closed-loop stability margin of vehicular platoons," *IEEE Transactions on Automatic Control*, vol. 54, pp. 2100–2113, Sep. 2009.
- [12] Y. Zhang, B. Kosmatopoulos, P. A. Ioannou, and C. C. Chien, "Using front and back information for tight vehicle following maneuvers," *IEEE Transactions on Vehicular Technology*, vol. 48, pp. 319–328, Jan 1999.
- [13] F. Lin, M. Fardad, and M. R. Jovanovic, "Optimal control of vehicular formations with nearest neighbor interactions," *IEEE Transactions on Automatic Control*, vol. 57, pp. 2203–2218, Sep. 2012.
- [14] K.-c. Chu, "Decentralized control of high-speed vehicular strings," *Transportation Science*, vol. 8, no. 4, pp. 361–384, 1974.
- [15] P. J. Seiler, "Coordinated control of unmanned aerial vehicles," 2001.
- [16] H. Raza and P. Ioannou, "Vehicle following control design for automated highway systems," *IEEE Control Systems Magazine*, vol. 16, no. 6, pp. 43–60, 1996.
- [17] Y. Sugiyama, M. Fukui, M. Kikuchi, K. Hasebe, A. Nakayama, K. Nishinari, S. ichi Tadaki, and S. Yukawa, "Traffic jams without bottlenecks—experimental evidence for the physical mechanism of the formation of a jam," 2008.
- [18] S. Cui, B. Seibold, R. Stern, and D. B. Work, "Stabilizing traffic flow via a single autonomous vehicle: Possibilities and limitations," in *2017 IEEE Intelligent Vehicles Symposium (IV)*, pp. 1336–1341, June 2017.
- [19] Y. Zheng, J. Wang, and K. Li, "Smoothing traffic flow via control of autonomous vehicles," *arXiv preprint arXiv:1812.09544*, 2018.
- [20] R. E. Stern, S. Cui, M. L. Delle Monache, R. Bhadani, M. Bunting, M. Churchill, N. Hamilton, H. Pohlmann, F. Wu, B. Piccoli, *et al.*, "Dissipation of stop-and-go waves via control of autonomous vehicles: Field experiments," *Transportation Research Part C: Emerging Technologies*, vol. 89, pp. 205–221, 2018.
- [21] M. Pooladsanj, K. Savla, and P. Ioannou, "Vehicle following over a closed ring road under safety constraint," in *2020 IEEE Intelligent Vehicles Symposium (IV)*, pp. 413–418, IEEE.
- [22] R. J. Caudill and W. L. Garrard, "Vehicle-follower, longitudinal control for automated transit vehicles," *IFAC Proceedings Volumes*, vol. 9, no. 4, pp. 195 – 209, 1976. IFAC/IFIP/IFORS 3rd International Symposium on Control in Transportation Systems, Columbus, Ohio, 9-13 August.
- [23] S. E. Sheikholeslam, *Control of a Class of Interconnected Nonlinear Dynamical Systems: The Platoon Problem*. PhD thesis, EECs Department, University of California, Berkeley, 1991.
- [24] V. Milanés, S. E. Shladover, J. Spring, C. Nowakowski, H. Kawazoe, and M. Nakamura, "Cooperative adaptive cruise control in real traffic situations," *IEEE Transactions on intelligent transportation systems*, vol. 15, no. 1, pp. 296–305, 2013.
- [25] H. K. Khalil and J. W. Grizzle, *Nonlinear systems*, vol. 3. Prentice hall Upper Saddle River, NJ, 2002.